Random front propagation
in fractional diffusive systems

Andrea Mentrelli[1,2], Gianni Pagnini[2,3]

[1]*Department of Mathematics & Alma Mater Research Center on Applied Mathematics –*
(AM)[2],
University of Bologna, via Saragozza 8, 40123 Bologna, Italy
andrea.mentrelli@unibo.it

[2]*BCAM – Basque Center for Applied Mathematics*
Alameda de Mazarredo 14, E48009 Bilbao, Basque Country – Spain

[3]*Ikerbasque – Basque Foundation for Science*
Calle de María Díaz de Haro 3, E48013 Bilbao, Basque Country – Spain
gpagnini@bcamath.org

Dedicated to Professor Francesco Mainardi
on the occasion of his retirement

Communicated by Enrico Scalas

Abstract

Modelling the propagation of interfaces is of interest in several fields of applied sciences, such as those involving chemical reactions where the reacting interface separates two different compounds. When the front propagation occurs in systems characterized by an underlying random motion, the front gets a random character and a tracking method for fronts with a random motion is desired. The Level Set Method, which is a successful front tracking technique widely used for interfaces with deterministic motion, is here randomized assuming that the motion of the interface is characterized by a random diffusive process. In particular, here we consider the case of a motion governed by the time-fractional diffusion equation, leading to a probability density function for the interface particle displacement given by the M-Wright/Mainardi function. Some numerical results are shown and discussed.

Keywords: `random front propagation, level set method, time-fractional diffusion, M-Wright/Mainardi function.`

AMS subject classification: `60G22, 60K37, 35F21, 65M08`

1. Introduction.

Tracking fronts and interfaces is a fundamental task in several real world applications of mathematical modelling. One of the most widely used and

successful tool for this purpose is the Level Set Method (LSM) [1,2], which has been adopted in many different problems, including, for example, turbulent premixed combustion [3] (to solve the so-called as G-equation [4]), wildland fire propagation [5], groundwater infiltration [6], biology [7] and material science [8].

Originally introduced by Osher and Sethian [1], the LSM is a highly robust and accurate method for tracking interfaces in any spatial dimension. The motion of the propagating surface is governed by Hamilton–Jacobi equations. Since in this setting sharp gradients and cusps can be easily accounted for and the effects of curvature may be easily incorporated as well, the LSM is particularly useful to handle problems in which the speed of the evolving interface is dependent on the interface properties, such as curvature and normal direction, as well as on the boundary conditions at the interface location. Hence, it is suitable for problems in which the topology of the evolving interface changes during the events, as when topological merging and breaking naturally occur.

However, even if the LSM is a technique with strong theoretical [1,2,9] and numerical [10,11] basis, in many applications the front is embedded into a random environment and therefore the interface gets a random character. An approach to "randomize" and average the LSM is needed.

Here, we consider an approach for tracking random fronts that is based on the idea to consider the interface as embodied by particles with random motion. This approach, first proposed to model turbulent premixed combustion [12], has also been recently applied to wildland fire propagation [13–17].

In the proposed model, the front position is assumed to be split into a deterministic part and a fluctuating part. According to this split, the deterministic position of the particles, and then of the interface, is assumed to be given by the ordinary LSM while a probability density function (PDF) describes the particle spreading around the deterministic position because of the random nature of the underlying environment. The average front emerges to be determined by the weighted superposition of the solutions of the ordinary LSM with the particle PDF as a weight function. This formulation being based on the LSM has the same remarkable property to be compatible with every type of geometry and flow in a simpler and more versatile way than previous approaches, and it emerges to be easily modifiable to include more detailed and correct physics.

The resulting evolution equation for the average value of the observable turns out to be a reaction-diffusion equation. The modelling approach based on reaction-diffusion equations and the one based on LSM can be considered alternative to each other because the solution of the reaction-diffusion

equation is generally a continuous smooth function that has an exponential decay and an infinite support, while the LSM generates a sharp function with a finite support. However, these two approaches are indeed reconciled in the proposed method resulting in the fact that, when the LSM is developed for tracking an interface with a random motion, the averaged process emerges to be governed by an evolution equation of reaction-diffusion type. In this reconciled approach, the front speed keeps the same key and characterizing role proper to the LSM.

The study of front propagation is important in chemically reactive systems. The reaction rates are dependent on the average values of the reactant density. In a diffusive media, reactant concentrations depends on diffusion properties. In the present study, it is considered the propagation of a plane front embedded into an environment characterized by subdiffusion as modelled by the time-fractional diffusion equation. Thus a one-dimensional problem is investigated and the particle PDF follows to be related to the M-Wright/Mainardi function.

The paper is organized as follows. In Section 2 the LSM is briefly reviewed focusing on its key basic properties. In Section 3, the main features of the "randomized" LSM, first introduced in [12], are recalled. The PDF of the displacement of the interface particles, which appears as a consequence of their random motion, is here assumed to be connected to anomalous diffusion phenomena. In Section 4 the pertinent time-fractional diffusion equation is discussed as long as its basic features in the one-, two- and three-dimensional cases. In Section 5, a selection of the obtained numerical results concerning one-dimensional front propagation in presence of anomalous diffusion with subdiffusive feratures is presented and discussed. Finally, in Section 6 the conclusions of the present study are drawn and its future developments are outlined.

2. The Level Set Method.

The LSM has been designed to track an interface in frameworks with a clear distinction between the interior and exterior part of the domain. This method can be briefly described in two dimensions as follows. Let Γ be a simple closed curve, or an ensemble of simple non-intersecting closed curves, representing a propagating interface in two dimensions, and let $\gamma : \mathcal{S} \times [0, +\infty[\to \mathbb{R}$ be a function defined on the domain of interest $\mathcal{S} \subseteq \mathbb{R}$ such that the level set $\gamma(\mathbf{x}, t) = \gamma_*$ coincides with the evolving front, i.e. $\Gamma(t) = \{\mathbf{x} \in \mathcal{S} \mid \gamma(\mathbf{x}, t) = \gamma_*\}$. In the case of a non-simply connected domain including n simply connected subdomains, the considered *interface* Γ is the ensemble of n curves surrounding each simply connected subdomain.

The evolution of the field $\gamma(\mathbf{x}, t)$ is governed by the following Hamilton–Jacobi equation [2]

$$\frac{\partial \gamma}{\partial t} = \mathcal{V}(\mathbf{x}, t) \left\| \nabla \gamma \right\|, \quad \gamma(\mathbf{x}, t = 0) = \gamma_0(\mathbf{x}),$$

(1)

which is the *ordinary* level set equation, where γ_0 is the initial field embedding the interface Γ at $t = 0$, i.e. $\Gamma_0 \equiv \Gamma(t = 0)$.

The function $\gamma(\mathbf{x}, t)$ can be called *level set function* and the quantity $\mathcal{V}(\mathbf{x}, t)$, which has the dimension of a velocity, can be identified as the Rate Of Spread (ROS) and its determination is problem dependent.

The subsets of the domain $\mathcal{S}$ corresponding to the interface Γ and to the region Ω enclosed by Γ (which represent, respectively, the interface and the domain bounded by it) may be conveniently described by the two indicator functions $\mathcal{I}_\Gamma, \mathcal{I}_\Omega : \mathcal{S} \times [0, +\infty[\to \{0, 1\}$ defined as follows:

$$\mathcal{I}_\Gamma(\mathbf{x}, t) = \begin{cases} 1, & \text{if } \gamma(\mathbf{x}, t) = \gamma_* \\ \\ 0, & \text{elsewhere} \end{cases},$$

(2)

and

$$\mathcal{I}_\Omega(\mathbf{x}, t) = \begin{cases} 1, & \text{if } \gamma(\mathbf{x}, t) \leqslant \gamma_* \\ \\ 0, & \text{elsewhere} \end{cases}.$$

(3)

The indicator functions at time $t = 0$, i.e. $\mathcal{I}_\Gamma(\mathbf{x}, t = 0)$ and $\mathcal{I}_\Omega(\mathbf{x}, t = 0)$, are denoted in the following as $\mathcal{I}_{\Gamma_0}(\mathbf{x})$ and $\mathcal{I}_{\Omega_0}(\mathbf{x})$, respectively.

In the case of an interface Γ made up of n closed curves, the domain Ω results to be a non-simply connected domain including n simply connected subdomains that independently evolves.

3. Model picture and mathematical formulation.

Similarly to the Eulerian and Lagrangian view points in fluid mechanics, we consider now the motion of the particles that made up the interface. Let the motion of each interface particle be random. For any realization indexed by ω, the random trajectory of these particles is stated to be $\mathbf{X}^\omega(t, \overline{\mathbf{x}}_0)$ with the same fixed initial condition $\mathbf{X}^\omega(0, \overline{\mathbf{x}}_0) = \overline{\mathbf{x}}_0$ in all realizations. By using statistical mechanics formalism [18], the trajectory of a single interface particle is marked out by the one-particle density function $p^\omega(\mathbf{x}; t) = \delta(\mathbf{x} - \mathbf{X}^\omega(t, \overline{\mathbf{x}}_0))$, where $\delta(\mathbf{x})$ is the Dirac δ-function.

The deterministic level set function γ, which is solution of Equation (1), may be written as

$$\gamma\left(\mathbf{x}, t\right) = \int_{\mathcal{S}} \gamma\left(\overline{\mathbf{x}}, t\right) \, \delta\left(\mathbf{x} - \overline{\mathbf{x}}\right) \, d\overline{\mathbf{x}}. \tag{4}$$

Let γ^ω be the random level set function corresponding the ω-realization that embeds the frontline Γ^ω. The equation analog of (4) turns out to be:

$$\gamma^\omega(\mathbf{x}, t) = \int_{\mathcal{S}} \gamma(\overline{\mathbf{x}}, t) \, \delta(\mathbf{x} - \mathbf{X}^\omega(t, \overline{\mathbf{x}})) \, d\overline{\mathbf{x}}. \tag{5}$$

Accordingly, $\mathcal{I}_\Gamma$ and $\mathcal{I}_\Omega$ are replaced by the new indicator functions $\mathcal{I}_{\Gamma^\omega}, \mathcal{I}_{\Omega^\omega} : \mathcal{S} \times [0, +\infty[\to \{0, 1\}$ defined as follows:

$$
\begin{aligned}
\mathcal{I}_{\Gamma^\omega}(\mathbf{x}, t) &= \int_{\mathcal{S}} \mathcal{I}_{\Gamma_0}(\overline{\mathbf{x}}_0) \, \delta(\mathbf{x} - \mathbf{X}^\omega(t, \overline{\mathbf{x}}_0)) \, d\overline{\mathbf{x}}_0 \\
&= \int_{\Gamma_0} \delta(\mathbf{x} - \mathbf{X}^\omega(t, \overline{\mathbf{x}}_0)) \, d\overline{\mathbf{x}}_0 \\
&= \int_{\Gamma(t)} \delta(\mathbf{x} - \mathbf{X}^\omega(t, \overline{\mathbf{x}})) \, d\overline{\mathbf{x}}
\end{aligned} \tag{6}
$$

and

$$
\begin{aligned}
\mathcal{I}_{\Omega^\omega}(\mathbf{x}, t) &= \int_{\mathcal{S}} \mathcal{I}_{\Omega_0}(\overline{\mathbf{x}}_0) \, \delta(\mathbf{x} - \mathbf{X}^\omega(t, \overline{\mathbf{x}}_0)) \, d\overline{\mathbf{x}}_0 \\
&= \int_{\Omega_0} \delta(\mathbf{x} - \mathbf{X}^\omega(t, \overline{\mathbf{x}}_0)) \, d\overline{\mathbf{x}}_0 \\
&= \int_{\Omega(t)} \delta(\mathbf{x} - \mathbf{X}^\omega(t, \overline{\mathbf{x}})) \, d\overline{\mathbf{x}},
\end{aligned} \tag{7}
$$

where, for any fixed initial condition $\overline{\mathbf{x}}_0$, the evolution of the deterministic trajectory is denoted by $\overline{\mathbf{x}}(t)$ and it is obtained uniquely by a deterministic time-reversible map $\overline{\mathbf{x}}(t) = \mathcal{F}(t, \overline{\mathbf{x}}_0)$. Moreover, an incompressibility-like condition can be assumed. The meaning is that the number of particles embodying the interface is kept constant while the the frontline enlarges. Thus the Jacobian J of the motion law is $J = d\overline{\mathbf{x}}_0/d\overline{\mathbf{x}} = 1$.

Hence, denoting by $\langle \cdot \rangle$ the ensemble average, the *effective indicator* of the region surrounded by an random front, $\varphi_e(\mathbf{x}, t) : \mathcal{S} \times [0, +\infty[\to [0, 1]$,

may be defined as:

$$\varphi_e(\mathbf{x}, t) = \langle \mathcal{I}_{\Omega^\omega(t)} \rangle = \langle \int_{\Omega(t)} \delta(\mathbf{x} - \mathbf{X}^\omega(t, \overline{\mathbf{x}}))\, d\overline{\mathbf{x}} \rangle$$

$$= \int_{\Omega(t)} \langle \delta(\mathbf{x} - \mathbf{X}^\omega(t, \overline{\mathbf{x}})) \rangle\, d\overline{\mathbf{x}}$$

(8)
$$= \int_{\Omega(t)} p(\mathbf{x}; t | \overline{\mathbf{x}})\, d\overline{\mathbf{x}}\,,$$

where $p(\mathbf{x}; t | \overline{\mathbf{x}}) = \langle \delta(\mathbf{x} - \mathbf{X}^\omega(t, \overline{\mathbf{x}})) \rangle$ is the PDF of the displacement of the interface particles around the average position $\overline{\mathbf{x}}$. Equation (8) has been originally proposed to model the burned mass fraction in turbulent premixed combustion [12].

Since the present approach is formulated to study the effects of an underlying diffusive media in front propagation processes, according to classical properties of diffusion, the resulting PDF $p(\mathbf{x}; t | \overline{\mathbf{x}})$ of the stochastic process $\mathbf{X}^\omega$ is considered to be unimodal and its mean and median are coincident. This means that $p(\mathbf{x}; t | \overline{\mathbf{x}})$ is a symmetric probability distribution which normalizes after integration both over $\mathbf{x}$ and $\overline{\mathbf{x}}$. Consequently, values of the *effective indicator* $\varphi_e(\mathbf{x}, t)$ range in the compact interval $[0, 1]$.

It should be noted that the *effective indicator* φ_e introduced here is not an indicator function in the classical sense. In fact, adopting the language of fuzzy logic, it is properly a *membership function*, being its range the compact interval $[0, 1]$ rather than the discrete set $\{0, 1\}$. Despite this, since the concept of probability which led to Equation (8) should not be confused with the concept of degree of truth (typical of fuzzy logic), φ_e is classified as an indicator function instead of a membership function.

Making use of the indicator function $\mathcal{I}_\Omega$, Equation (8) can be further written as:

(9)
$$\varphi_e(\mathbf{x}, t) = \int_{\mathcal{S}} \mathcal{I}_\Omega(\overline{\mathbf{x}}, t)\, p(\mathbf{x}; t | \overline{\mathbf{x}})\, d\overline{\mathbf{x}}\,.$$

It is worth noting that the deterministic trajectory $\overline{\mathbf{x}}$ is the trajectory of a point belonging to the ordinary level set contour with the same initial condition $\overline{\mathbf{x}}_0$. In the deterministic case, i.e. $\mathbf{X}^\omega(t, \overline{\mathbf{x}}) = \overline{\mathbf{x}}$ for all realizations, it turns out that $p(\mathbf{x}; t | \overline{\mathbf{x}}) = \delta(\mathbf{x} - \overline{\mathbf{x}})$, and from Equation (9) one recovers $\varphi_e(\mathbf{x}, t) = \mathcal{I}_{\Omega(t)}$.

Applying the Reynolds transport theorem to Equation (8), the evolution equation of the effective indicator $\varphi_e(\mathbf{x}, t)$ becomes [12]:

(10)
$$\frac{\partial \varphi_e}{\partial t} = \int_{\Omega(t)} \frac{\partial p}{\partial t}\, d\overline{\mathbf{x}} + \int_{\Omega(t)} \nabla_{\overline{\mathbf{x}}} \cdot [\mathbf{V}(\overline{\mathbf{x}}, t)\, p(\mathbf{x}; t | \overline{\mathbf{x}})]\, d\overline{\mathbf{x}}\,,$$

where $\mathbf{V}(\overline{\mathbf{x}}, t) = \mathcal{V}(\overline{\mathbf{x}}, t)\,\hat{\mathbf{n}}$, with $\hat{\mathbf{n}} = -\nabla\gamma/\|\nabla\gamma\|$, with reference to Equation (1). For a deterministic motion, i.e. when $p(\mathbf{x}; t|\overline{\mathbf{x}}) = \delta(\mathbf{x}-\overline{\mathbf{x}})$, Equation (10) reduces to the ordinary level set equation (1) [12].

Since the range of the effective indicator φ_e is the compact interval $[0, 1]$, a criterion to mark the *effective* surrounded region Ω_e has to be stated. In particular, here we mark when the effective indicator exceeds an arbitrarily fixed threshold value φ_e^{th}, i.e. $\Omega_e(\mathbf{x}, t) = \{\mathbf{x} \in \mathcal{S} \mid \varphi_e(\mathbf{x}, t) > \varphi_e^{th}\}$.

4. The time-fractional diffusion equation.

The random trajectory of each interface particle is assumed to be determined as $\mathbf{X}^\omega(t, \mathbf{x}) = \overline{\mathbf{x}}_{ROS} + \chi^\omega$, where $\overline{\mathbf{x}}_{ROS}$ is a deterministic position defined as $d\overline{\mathbf{x}}_{ROS}/dt = \mathbf{V}(\overline{\mathbf{x}}_{ROS}, t)$ and χ is the noise corresponding to the underlying diffusive environment.

When the system is characterized by anomalous diffusion, the evolution in time of particle PDF can be modelled by the *time-fractional diffusion equation*, which is obtained from the diffusion equation by replacing the first order time derivative with a real order derivative operator [19–21]. This replacement can be done by using the time fractional derivative operator in the Caputo sense or in the Riemann–Liouville sense. However, these two forms are equivalent if standard initial condition is used [22].

The emergence of fractional kinetics in complex media has been recently described within the standard diffusion framework in terms of parameter fluctuations [23].

Let β be a real positive parameter limited as $0 < \beta \le 1$, the time-fractional diffusion equation in the Caputo sense reads

$$(11) \qquad {}_*D_t^{2\beta}u = K\,\nabla^2 u\,,$$

where coefficient K is a positive constant with dimensions $[K] = [L]^2[T]^{-2\beta}$ and ${}_tD_*^\mu$ is the *Caputo* fractional derivative defined for a sufficiently well-behaved function $f(t)$ by its Laplace transform as

$$(12) \qquad \int_0^{+\infty} \mathrm{e}^{-st}\,\{{}_tD_*^\mu f(t)\}\,dt = s^\mu\,\widetilde{f}(s) - \sum_{k=0}^{m-1} s^{\mu-1-k}\,f^{(k)}(0^+)\,,$$

with $m - 1 < \mu \le m$ and $m \in N$.

The time-fractional diffusion equation in the Riemann–Liouville sense reads

$$(13) \qquad \frac{\partial u}{\partial t} = K\,D_t^{1-2\beta}\,\nabla^2 u\,,$$

where D^μ is the Riemann–Liouville fractional derivative defined as

$$(14) \qquad \int_0^{+\infty} e^{-st} \{_t D^\mu f(t)\} \, dt = s^\mu \, \widetilde{f}(s) \,,$$

provided that all the limiting values $f^{(k)}(0^+)$ are finite with $k \in N$ such that $0 \leq k \leq m - 1$ where $m \in N$ and $m - 1 < \mu \leq m$.

When $\beta = 0.5$ Equations (11) and (13) become the normal diffusion equation and when $\beta = 1$ they reduce to wave equation.

Green's function $\mathcal{G}$ of Equations (11) and (13) for arbitrary dimension d is [21]

$$(15)$$
$$\mathcal{G}_{\mathrm{d}}(\mathbf{x};t) = \frac{1}{(2\pi)^{d/2+1} i K^{(1+d/2)/2}} \int_{-i\infty}^{+i\infty} s^{\beta(d/2+1)-1} \, e^{st} \, \mathcal{K}_{d/2-1}(s^\beta r/\sqrt{K}) \, ds \,,$$

where $\mathcal{K}_\nu$ is the Macdonald function, or modified Bessel function of the second kind, of order ν and $r = |\mathbf{x}|$. Moreover, $\mathcal{G}_{\mathrm{d}}$ is real by setting $s = -i\omega$, $\omega \in R$, and then $s^\beta = e^{-i\pi\beta \, \mathrm{sgn}\,\omega/2}|\omega|^\beta$ [21].

In one and three dimensional cases, Green's function (15) can be expressed in terms of the M-Wright function M_β [21] as

$$(16)$$
$$\mathcal{G}_{\mathrm{1D}}(x;t) = \frac{1}{2} \frac{1}{\sqrt{K}\, t^\beta} M_\beta\left(\frac{|x|}{\sqrt{K}\, t^\beta}\right) \,, \quad \mathcal{G}_{\mathrm{3D}}(x;t) = -\frac{1}{2\pi r} \frac{\partial}{\partial r} \mathcal{G}_{\mathrm{1D}}(r;t) \,.$$

To have a proper diffusion process characterized by a unimodal PDF, parameter β must be constrained as $0 < \beta < 1/2$ [19,24], from which sub-diffusion follows. Furthermore, from (16) it follows also that when $1/2 < \beta < 1$, since the function $M_\beta(z)$ is bimodal, the Green function $\mathcal{G}_{\mathrm{3d}}$ can be negative and no kind of diffusion occurs.

Function $M_\nu(z)$, $0 < \nu < 1$, is called M-Wright/Mainardi function [25–28], its series representation is

$$(17) \quad M_\nu(z) = \sum_{n=0}^\infty \frac{(-z)^n}{n!\,\Gamma[-\nu n + (1-\nu)]} = \frac{1}{\pi} \sum_{n=1}^\infty \frac{(-z)^{n-1}}{(n-1)!}\, \Gamma(\nu n)\, \sin(\pi\nu n) \,,$$

and a noteworthy particular case is

$$(18) \qquad M_{1/2}(z) = \frac{1}{\sqrt{\pi}} \exp\left(-z^2/4\right) \,.$$

In spite of the fact that for some particular properties the $M_\nu(z)$ can be considered a *generalized hyper-Airy function* [29], in view of its leading role

in diffusive stochastic processes, it is now considered as a natural (fractional) generalization of the Gaussian function [30]. Further properties on the M-Wright function can be found in the book by Mainardi [31], especially in Chapter 6 and Appendix F.

The subdiffusive character is highlighted by particle variance that in one dimension is [21,24]

$$(19) \qquad \sigma_{1\mathrm{d}}^2 = \int_{-\infty}^{+\infty} x^2 \, \mathcal{G}_{1\mathrm{d}}(x;t) \, dx = \frac{2}{\Gamma(2\beta+1)} \, K \, t^{2\beta} \,,$$

so that $\sigma_{2\mathrm{d}}^2 = 2\,\sigma_{1\mathrm{d}}^2$ and $\sigma_{3\mathrm{d}}^2 = 3\,\sigma_{1\mathrm{d}}^2$ [21].

Readers interested on the time-fractional diffusion equation can find a deeper analysis for example in References [24,32,33].

Since $\mathcal{G}_{\mathrm{d}}(\mathbf{x};t)$ is a symmetric probability distribution (i.e. $\mathcal{G}_{\mathrm{d}}(\mathbf{x};t) = \mathcal{G}_{\mathrm{d}}(|\mathbf{x}|;t)$, see (15)) and also unimodal, then the mode, the mean and the median coincide such that for a given average value $\overline{\mathbf{x}}$ it holds $\mathcal{G}_{\mathrm{d}}(\mathbf{x};t|\overline{\mathbf{x}}) = \mathcal{G}_{\mathrm{d}}(\mathbf{x} - \overline{\mathbf{x}};t)$. Finally, in the time-fractional diffusion case here considered, Equation (9) results to be

$$(20) \qquad \varphi_e(\mathbf{x},t) = \int_{\mathcal{S}} \mathcal{I}_{\Omega}(\overline{\mathbf{x}},t) \, \mathcal{G}_{\mathrm{d}}(\mathbf{x} - \overline{\mathbf{x}};t) \, d\overline{\mathbf{x}} \,,$$

and, by using (13), evolution equation (10) turns out to be

$$\frac{\partial \varphi_e}{\partial t} = \int_{\Omega(t)} \frac{\partial \mathcal{G}_{\mathrm{d}}}{\partial t} \, d\overline{\mathbf{x}} + \int_{\Omega(t)} \nabla_{\overline{\mathbf{x}}} \cdot [\mathbf{V}(\overline{\mathbf{x}},t) \, \mathcal{G}_{\mathrm{d}}(\mathbf{x} - \overline{\mathbf{x}};t)] \, d\overline{\mathbf{x}}$$

$$(21) \quad = K \, \nabla^2 \int_{\Omega(t)} D_t^{1-2\beta} \, \mathcal{G}_{\mathrm{d}}(\mathbf{x} - \overline{\mathbf{x}};t) \, d\overline{\mathbf{x}} + \int_{\Omega(t)} \nabla_{\overline{\mathbf{x}}} \cdot [\mathbf{V}(\overline{\mathbf{x}},t) \, \mathcal{G}_{\mathrm{d}}(\mathbf{x} - \overline{\mathbf{x}};t)] \, d\overline{\mathbf{x}} \,.$$

Numerical solutions of formula (20) are discussed in the following section.

5. Numerical results.

In this section, a selection of the numerical results obtained for the propagation of fronts in presence of anomalous diffusion, as well as normal diffusion, is proposed. The results are here limited to the one-dimensional case, involving the propagation of plane fronts, the analysis in two and three dimensions is presented elsewhere [34]. The one-dimensional case, despite its simplicity, has the relevant advantage to easily allow to point out the main features of the front propagation when diffusion processes come into play, and to help in performing a straightforward comparison between the effects of normal and anomalous diffusion on the front propagation.

The numerical results have been obtained by means of a software package suitably developed for the purpose. This includes a Python/Fortran95 library (`pyMlib`) useful for the numerical computation of the fundamental solutions in the one-, two-, and three-dimensional cases by means of several state-of-the-art algorithms [21,35], and is coupled with a standard LSM library [36].

The one-dimensional fundamental solution for the various values of the parameter β, ranging from $\beta = 0.1$ to $\beta = 0.5$, that will be considered throughout this section is represented in Fig. 1. It is worth recalling here that the case with $\beta = 0.5$ coincides with the case of normal diffusion, while the cases with $0 < \beta < 0.5$ are associated to anomalous diffusion and, in particular, model the so-called "subdiffusive" phenomena.
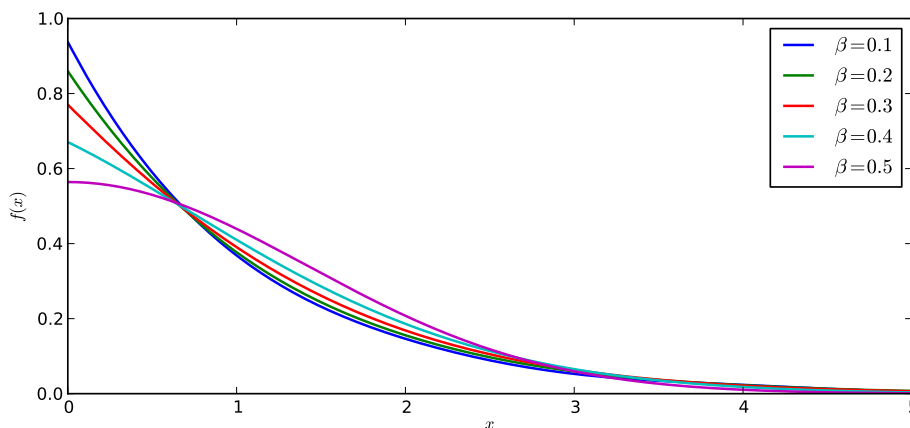
Figure 1.   Fundamental solution in the one-dimensional case for five values of the parameter β: $\beta = 0.1$, 0.2, 0.3, 0.4, 0.5, where $\beta = 0.5$ corresponds to the case of normal diffusion.

The analysis proposed here focuses on the investigation of the combined effects of the diffusion coefficient K and of the parameter β on the features of the random propagating front.

When the diffusion coefficient K is *small* enough, one can see that – no matter the value of the coefficient β – the only outstanding feature of the propagating front is its smoothing with respect to the sharp front obtained in the deterministic (non-diffusive) case. The profiles plotted in Fig. 2, in which the numerically computed random fronts are plotted together with the deterministic front for the case $K = 5$, are representative of this behaviour.

On contrast, when the diffusion coefficient K is *large*, the qualitative

10
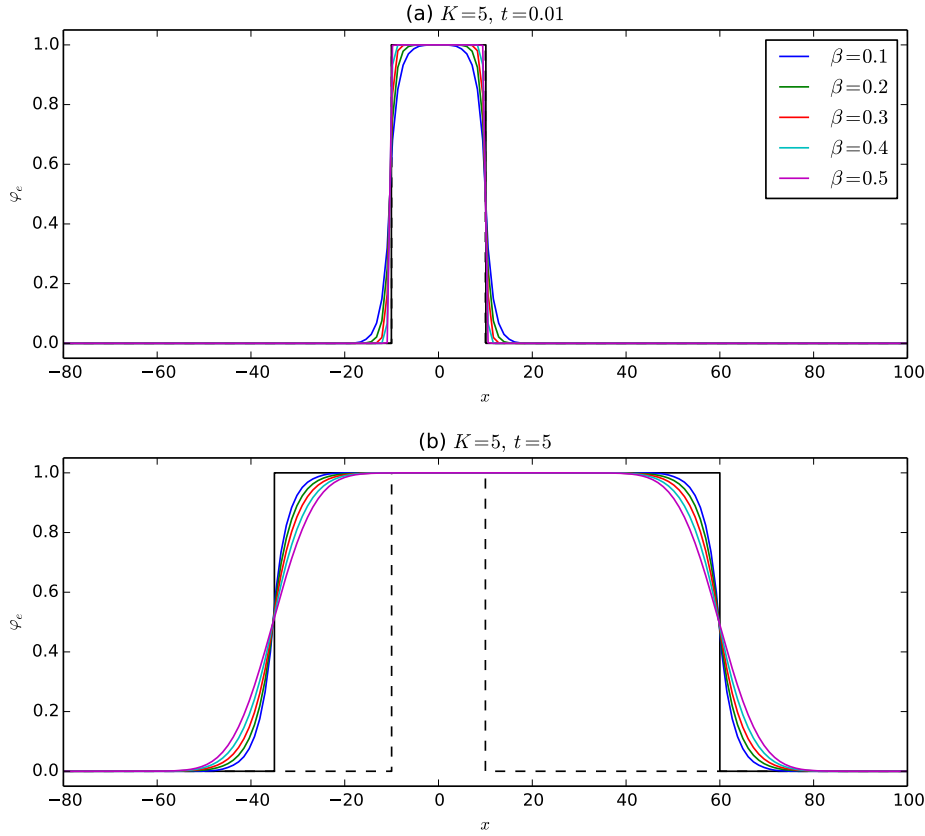
Figure 2. Evolution of the deterministic front (black curve) and of random fronts for several values of β (coloured curves) for $K = 5$ for two time instants: (a) $t = 0.01$ and (b) $t = 5$. All the fronts are located at $t = 0$ in $x = x_l = -10$ and $x = x_r = 10$ (dotted line) and they propagate to the right with velocity $v_l = -5$ and to the left with velocity $v_l = 10$.

behaviour of the random fronts is remarkably different from the behaviour reported in Fig. 2. In fact, as it is shown in Fig. 3, in this case the smoothing of the front may affect the existence of the bulk of the region Ω_e enclosed by the propagating front, where the "bulk region" is intended as the region characterized by φ_e close to 1. In this scenario, the maximum value of the effective indicator φ_e can be substantially reduced from its maximum unitary value, especially when the region Ω_e enclosed by the propagating front is small enough (i.e. for *small* times), leading to what may be referred to as a *weakening* effect of the diffusion phenomena on the region Ω_e. For *large* times, as the region enclosed by the propagating front increases in

11

size, the qualitative behaviour previously discussed for the case of a *small* diffusion parameter K can be eventually recovered, as it is seen in Fig. 3(c).

A remarkable feature of the random fronts connected with the anomalous diffusion phenomena, easily appreciable in the set of plots of Fig. 3, is that the more the diffusion is subdiffusive (i.e. the smaller is β), the more important the described weakening effect is. This effect, though, is seen only for small times: as time increases, the intrinsic subdiffusive nature of the diffusion emerges and the steepness of the random front increases, as expected, as the coefficient β decreases.

The features of the random fronts described so far for the case with $K = 100$ remains qualitatively unchanged as the diffusion coefficient K increases, but an important remark is in order. Depending on the physical interpretation of the indicator φ_e, it may – or may not – be meaningful to introduce the concept of an "effective" position of the propagating random front. In this cases, assuming the front to be located, say, at the position for which the effective indicator φ_e reaches the threshold value φ_e^{th}, it might be meaningful to argue that when the effective indicator φ_e is reduced to the extent as to be less of φ_e^{th} over all the domain Ω_e, the region Ω_e extinguishes and no further front propagation takes place. Such a circumstance may, for instance, be the case met in turbulent premixed combustion [12]: if φ_e marks the position of the propagating front, should the value of φ_e drop below the given threshold value, the flame would be regarded as extinguished and no further calculation of the front evolution would be meaningful. Accordingly to what already noticed, such a circumstance would become more and more likely as the diffusion coefficient K increases. In Fig. 4, one can see the propagation of the random and deterministic fronts obtained with $K = 500$. Assuming, for instance, $\varphi_e^{th} = 0.5$, in this case the area Ω_e associated with the front obtained with $\beta = 0.5$ (normal diffusion) would be extinguished already at $t = 5$ (see Fig. 4(b)), and any further calculation concerning the propagation of the connected random front would be meaningless, even if at larger times the effects of the diffusion would be such that the values of the effective indicator φ_e could reach values larger than the threshold φ_e^{th}, as seen if Fig. 4(c). However, as already noticed, these considerations are problem-dependent and strongly connected with the physical model under consideration.

The *weakening* effect of the diffusion on the size of the region Ω_e described above is well depicted in Fig. 5 and Fig. 6.

In Fig. 5(a) and Fig. 6(a), the ratio r of the sizes of the effective region Ω_e and of the deterministic region Ω (i.e the region associated with the deterministic front) is plotted as a function of time for the two cases, respectively of $K = 100$ and $K = 500$. It is evident that in the first case,
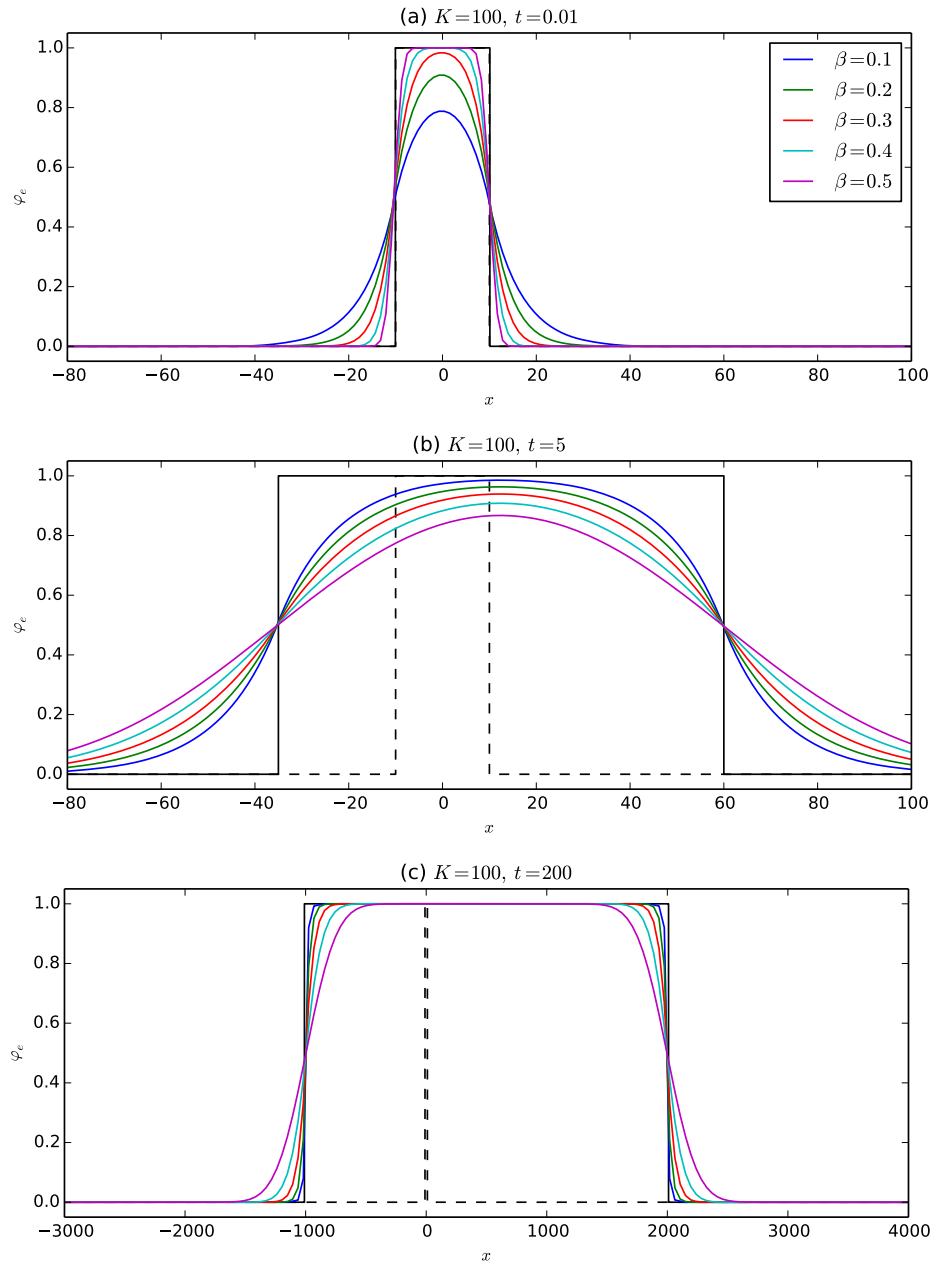
Figure 3. Evolution of the deterministic front (black curve) and of random fronts for several values of β (coloured curves) in the case of $K = 100$ at: (a) $t = 0.01$, (b) $t = 5$, (c) $t = 200$. The initial location and the velocities of the fronts are the same as in Figure 2.

13
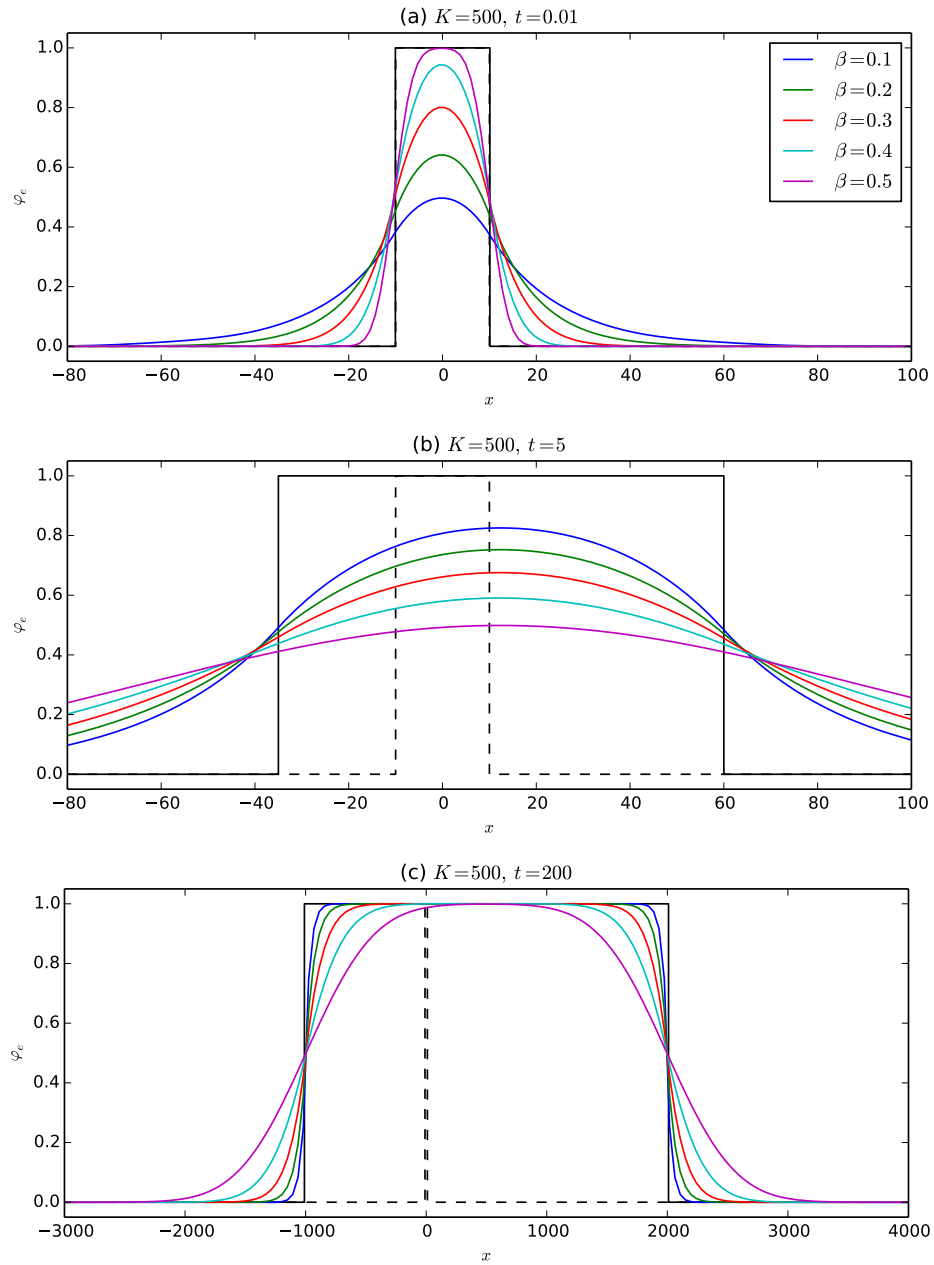
Figure 4. Evolution of the deterministic front (black curve) and of random fronts for several values of β (coloured curves) in the case of $K = 500$ at: (a) $t = 0.01$, (b) $t = 5$, (c) $t = 200$. The initial location and the velocities of the fronts are the same as in Figure 2.
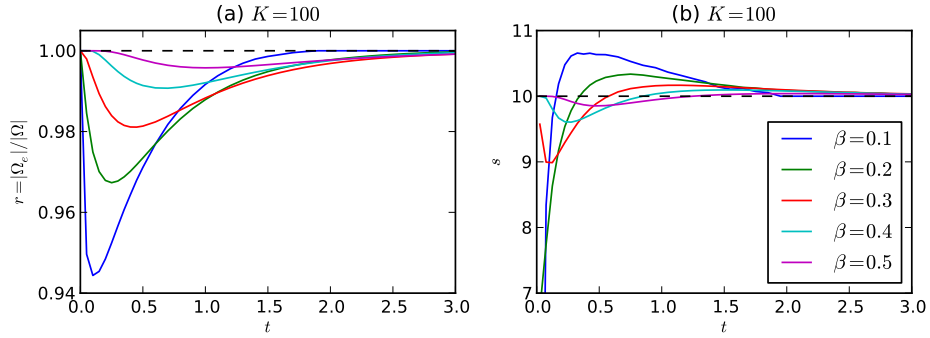
Figure 5. (a) Evolution of the ratio of the sizes of the effective region Ω_e and the deterministic region Ω, $r = \Omega_e/\Omega$, for several values of the parameter β in the case of a diffusion coefficient $K = 100$ and (b) corresponding front speeds. The fronts are supposed to be placed in the locations for which $\varphi_e^{th} = 0.5$.
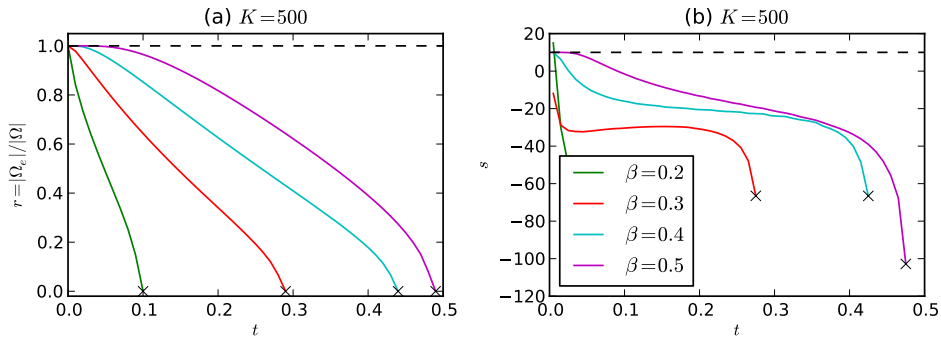
Figure 6. The same as in Fig. 5 but for $K = 500$. In this case, the regions Ω_e extinguish as a consequence of the weakening due to the diffusion. The crosses indicate the extinguishing of the regions Ω_e, corresponding to the time instant in which the maximum value of φ_e over all the domain falls below the threshold value $\varphi_e^{th} = 0.5$.

i.e. the case with $K = 100$ whose front profiles are plotted in Fig. 3, see Fig. 5(a), the region after being initially weakened as previously explained, eventually recovers reaching asymptotically a stable state. A completely different behaviour is, instead, shown in Fig. 6(a) for the case of $K = 500$: in this case, the diffusion is so strong that the weakening leads to the extinguishing of the region Ω_e. For the purpose of this analysis, all the fronts have been supposed to be located at the position for which $\varphi_e^{th} = 0.5$, and their velocities have been plotted as functions of time in Fig. 5(b) and Fig. 6(b).

6. Conclusions.

In this paper, a first step towards the development of a model and of the related numerical simulation set-up for the study of the propagation of interfaces whose particles are subject to random motion due to anomalous diffusion phenomena is presented.

To this purpose, the well-known LSM, which, in the past decades, has proven to be very successful in tracking the evolution of interfaces with complex motion, has been selected as the preferred tracking method. In its traditional formulation, the LSM accounts only for the motion of deterministic interfaces (i.e. interfaces whose particles' motion is deterministic), the introduction of a suitable generalization capable of accounting for a random motion of the interface particles is in order. This generalization, which has been here outlined following [12], is exploited in the case in which the PDF of the interface particle displacement is connected to the phenomena of anomalous diffusion taking place in the media in which the interface propagates.

The front propagation in presence of anomalous diffusion is then investigated, with the aid of numerical calculations carried out by means of a suitably developed code, in the one-dimensional case (plane fronts) under the restriction of subdiffusive phenomena.

The presented numerical results clearly show that when the intensity of the diffusion (namely, the diffusion coefficient K) is *small* enough, the propagating front is smoothed-out with respect to the sharp front obtained in the deterministic (non-diffusive) case, but the overall qualitative behaviour of the front propagation in not affected by the diffusive phenomena taking place in the medium. On contrast, when the intensity of the diffusion is *large*, the qualitative behaviour of the random fronts sensibly changes: in this case the smoothing of the front may be so significant as to even compromise the existence of the region enclosed by the propagating front (and the front itself, in turn). This effect, which has been referred to as a *weakening* effect of the diffusion phenomena on the region bounded by the propagating front can be, as shown, a transient effect gradually vanishing as the front propagates, or even a phenomenon which drastically affects the very existence of the front, depending on the intensity of the diffusion itself.

Moreover, aside from depending on the intensity of the diffusion phenomena through the diffusion coefficient K, the above-mentioned weakening effects has also been shown to be more pronounced as the subdiffusive nature of the diffusion increases.

The analysis presented here has been extended to the cases of two-dimensional as well as three-dimensional propagating interfaces and is pre-

sented elsewhere [34].

Acknowledgements.

REFERENCES

1. S. J. Osher and J. A. Sethian, Fronts propagating with curvature dependent speed: algorithms based on Hamilton–Jacobi formulations, *J. Comp. Phys.*, vol. 79, pp. 12–49, 1988.

2. J. A. Sethian and P. Smereka, Level set methods for fluid interfaces, *Ann. Rev. Fluid Mech.*, vol. 35, pp. 341–372, 2003.

3. D. Hartmann, M. Meinke, and W. Schröder, A level-set based adaptive-grid method for premixed combustion, *Combust. Flame*, vol. 158, pp. 1318–1339, 2011.

4. N. Peters, *Turbulent Combustion.* Cambridge: Cambridge University Press, 2004.

5. V. Mallet, D. E. Keyes, and F. E. Fendell, Modeling wildland fire propagation with level set methods, *Comput. Math. Appl.*, vol. 57, pp. 1089–1101, 2009.

6. E. Jettestuen, J. O. Helland, and M. Prodanović, A level set method for simulating capillary-controlled displacements at the pore scale with nonzero contact angles, *Water Resour. Res.*, vol. 49, pp. 4645–4661, 2013.

7. M. Machacek and G. Danuser, Morphodynamic profiling of protrusion phenotypes, *Biophys. J.*, vol. 90, pp. 1439–1452, 2006.

8. W. Guo and H. H. Sawin, Review of profile and roughening simulation in microelectronics plasma etching, *J. Phys. D: Appl. Phys.*, vol. 42, p. 194014, 2009.

9. J. A. Sethian, Curvature and the evolution of fronts, *Commun. Math. Phys.*, vol. 101, pp. 487–499, 1985.

10. J. A. Sethian, Numerical algorithms for propagating interfaces: Hamilton–Jacobi equations and conservation laws, *J. Diff. Geom.*, vol. 31, pp. 131–161, 1990.

11. J. A. Sethian, Numerical methods for propagating fronts, in *Variational*

Methods for Free Surface Interfaces (P. Concus and R. Finn, eds.), New York: Springer–Verlag, 1987.

12. G. Pagnini and E. Bonomi, Lagrangian formulation of turbulent pre-mixed combustion, *Phys. Rev. Lett.*, vol. 107, p. 044503, 2011.

13. G. Pagnini and L. Massidda, Modelling turbulence effects in wildland fire propagation by the randomized level-set method, Tech. Rep. 2012/PM12a, CRS4, July 2012. Revised Version August 2014. arXiv:1408.6129.

14. G. Pagnini and L. Massidda, The randomized level-set method to model turbulence effects in wildland fire propagation, in *Modelling Fire Behaviour and Risk. Proceedings of the International Conference on Fire Behaviour and Risk. ICFBR 2011, Alghero, Italy, October 4–6 2011* (D. Spano, V. Bacciu, M. Salis, and C. Sirca, eds.), pp. 126–131, May 2012. ISBN 978-88-904409-7-7.

15. G. Pagnini and A. Mentrelli, Modelling wildland fire propagation by tracking random fronts, *Nat. Hazards Earth Syst. Sci.*, vol. 14, pp. 2249–2263, 2014.

16. G. Pagnini, A model of wildland fire propagation including random effects by turbulence and fire spotting, in *Proceedings of XXIII Congreso de Ecuaciones Diferenciales y Aplicaciones XIII Congreso de Matemática Aplicada. Castelló, Spain, 9–13 September 2013*, pp. 395–403, 2013.

17. G. Pagnini, Fire spotting effects in wildland fire propagation, in *Advances in Differential Equations and Applications* (F. Casas and V. Martínez, eds.), vol. 4 of *SEMA SIMAI Springer Series*, pp. 203–214, Springer International Publishing Switzerland, 2014. DOI:10.1007/978-3-319-06953-1_20. ISBN: 978-3-319-06952-4. (eBook: 978-3-319-06953-1).

18. Y. L. Klimontovich, Nonlinear Brownian motion, *Physics-Uspekhi*, vol. 37, pp. 737–767, 1994.

19. F. Mainardi, Fractional relaxation-oscillation and fractional diffusion-wave phenomena, *Chaos Solitons Fract.*, vol. 7, pp. 1461–1477, 1996.

20. F. Mainardi, The fundamental solutions for the fractional diffusion-wave equation, *Appl. Math. Lett.*, vol. 9, no. 6, pp. 23–28, 1996.

21. A. Hanyga, Multidimensional solutions of time-fractional diffusion-wave equations, *Proc. R. Soc. Lond. A*, vol. 458, pp. 933–957, 2002.

22. F. Mainardi, G. Pagnini, and R. Gorenflo, Some aspects of fractional diffusion equations of single and distributed order, *Appl. Math. Comput.*, vol. 187, pp. 295–305, 2007.

23. G. Pagnini, Short note on the emergence of fractional kinetics, *Physica A*, vol. 409, pp. 29–34, 2014.

24. F. Mainardi, Y. Luchko, and G. Pagnini, The fundamental solution of the space-time fractional diffusion equation, *Fract. Calc. Appl. Anal.*, vol. 4, no. 2, pp. 153–192, 2001.

25. I. Podlubny, *Fractional Differential Equations*. San Diego: Academic Press, 1999.

26. R. Balescu, V-Langevin equations, continuous time random walks and fractional diffusion, *Chaos Solitons Fract.*, vol. 34, no. 1, pp. 62–80, 2007.

27. R. Metzler and J.-H. Jeon, Anomalous diffusion and fractional transport equations, in *Fractional Dynamics. Recent Advances* (S. C. Lim, J. Klafter, and R. Metzler, eds.), pp. 3–32, Singapore: World Scientific, 2012.

28. G. Pagnini and E. Scalas, Historical notes on the M-Wright/Mainardi function, *Commun. Appl. Math. Appl.*, vol. 6, pp. e–496, 2014. DOI:10.1685/journal.caim.496.

29. F. Mainardi and M. Tomirotti, On a special function arising in the time fractional diffusion-wave equation, in *Transform Methods and Special Functions, Sofia' 1994 (Proc. 1st Intern. Workshop)* (P. Rusev, I. Dimovski, and V. Kiryakova, eds.), pp. 171–183, Science Culture Technology, 1995.

30. G. Pagnini, The M-Wright function as a generalization of the Gaussian density for fractional diffusion processes, *Fract. Calc. Appl. Anal.*, vol. 16, no. 2, pp. 436–453, 2013.

31. F. Mainardi, *Fractional Calculus and Waves in Linear Viscoelasticity*. London: Imperial College Press, 2010.

32. F. Mainardi and G. Pagnini, The Wright functions as solutions of the time-fractional diffusion equation, *Appl. Math. Comput.*, vol. 141, no. 1, pp. 51–62, 2003.

33. W. R. Schneider and W. Wyss, Fractional diffusion and wave equations, *J. Math. Phys.*, vol. 30, no. 1, pp. 134–144, 1989.

34. A. Mentrelli and G. Pagnini, Front propagation in anomalous diffusive media, *J. Comp. Phys.*, vol. 293, pp. 427–441, 2014.

35. R. Gorenflo, J. Loutchko, and Y. Luchko, Computation of the Mittag–Leffler function $E_{\alpha,\beta}(z)$ and its derivative, *Fract. Calc. Appl. Anal.*, vol. 5, pp. 491–518, 2002.

36. K. T. Chu and M. Prodanović, Level set method library (LSMLIB), 2009. `http://ktchu.serendipityresearch.org/software/lsmlib/`.